



Determining the ultraviolet radiation dose experienced by aerosols using ultraviolet-sensitive dyes

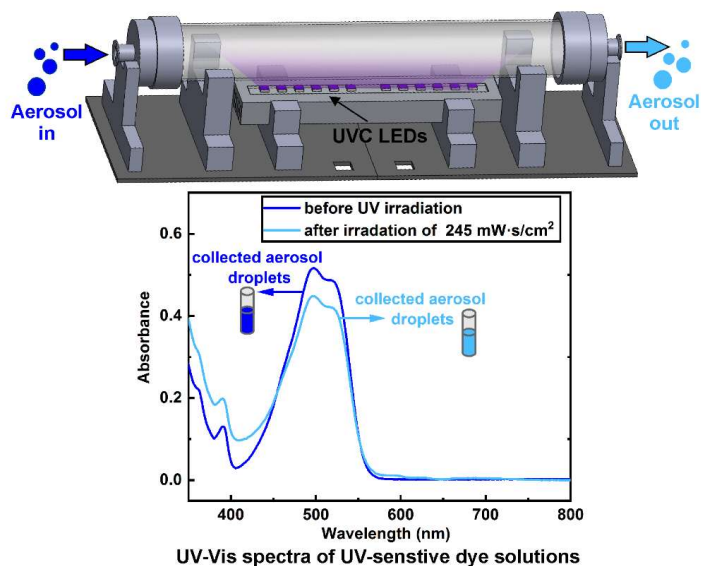
Qingqing Fu, Frank Einar Kruis

5 Institute of Technology for Nanostructures (NST) and Center for Nanointegration Duisburg-Essen (CENIDE);
Faculty of Engineering, University of Duisburg-Essen, Duisburg, 47057, Germany

Correspondence to: Frank Einar Kruis (einar.kruis@uni-due.de)

Keywords: viral aerosols, air disinfection, UVC radiation dose, ultraviolet-sensitive dyes, irradiation chamber

10 **Abstract.** The application of ultraviolet (UV)-based air disinfection holds promise, but also presents several
challenges. Among these, the quantitative determination of the required UV radiation dose for aerosols is
particularly significant. This study explores the possibility of determining the UV dose experienced by aerosols
without the use of virus-containing aerosols, circumventing associated laboratory safety issues. To achieve this,
15 we developed a model system comprised of UV-sensitive dyes dissolved in di-ethyl-hexyl-sebacate (DEHS),
which facilitates the generation of non-evaporating and UV-degradable aerosols. For the selection of UV-sensitive
dyes, 20 dyes were tested, and two of them were selected as most suitable according to several selection criteria.
Dye-laden aerosol droplets were generated using a commercial aerosol generator and subsequently exposed to
UVC radiation in a laboratory-built UV irradiation chamber. We designed a low-pressure impactor to collect the
20 aerosols pre- and post-UV exposure. Dye degradation, as a result of UV light exposure, was then analyzed by
assessing the concentration changes in the collected dye solutions using a UV-visible spectrophotometer. Our
findings revealed that a UV dose of $245 \text{ mW}\cdot\text{s}\cdot\text{cm}^{-2}$ resulted in a 10% degradation, while a lower dose of 21.6
 $\text{mW}\cdot\text{s}\cdot\text{cm}^{-2}$ produced a 5% degradation. In conclusion, our study demonstrates the feasibility of using aerosol
droplets containing UV-sensitive dyes to determine the UV radiation dose experienced by an aerosol.





1 Introduction

25 The COVID-19 pandemic, caused by the severe acute respiratory syndrome coronavirus 2 (SARS-CoV-2), has
profoundly impacted both individual lives and the global economy (Dong et al., 2020; Priya et al., 2021). The
predominant contributor to these effects is the rapid airborne transmission of the virus, often involving aerosols
smaller than five μm and traveling distances exceeding one to two meters from the infected individual (Zayas et
al., 2012; Wang et al., 2021; Lefebvre et al., 2022). A diverse, integrated approach has been implemented globally
30 in response to this pandemic. Public health measures such as the enforcement of personal protective equipment
(PPE) usage, including masks, adherence to social distancing guidelines, and promotion of hand hygiene practices,
have contributed to reducing viral transmission to some extent (Muñoz et al., 2021; Leung and Sun, 2020).
Vaccination serves as an essential strategy to control the COVID-19 pandemic because an effective vaccine could
induce an appropriate immune response. However, developing an effective vaccine is a time-consuming process
35 due to pre-clinical protocols and three-phase clinical trials necessary to ascertain safety and efficacy. Moreover,
environmental variations and differences in population densities across geographical areas can cause the viral
genome to mutate, allowing the virus to evade the immune system even after vaccination (Van Dorp et al., 2020;
Kaur and Gupta, 2020). Ultraviolet (UV) germicidal irradiation, specifically UVC irradiation within the
wavelength range of 200–280 nm (UVC), is known as an effective method for inactivating all known
40 microorganisms and viruses (Abkar et al., 2022; Inagaki et al., 2020; Reed, 2010; Biasin et al., 2021). UVC
radiation absorption results in the formation of dimeric lesions in the genome of pathogenic microorganisms, which
inhibit DNA/RNA replication and inactivate the pathogen (Mankar et al., 2022; Kim and Kang, 2018).
Furthermore, UV radiation presents a more environmentally friendly and energy-efficient alternative to liquid
disinfectants and heat disinfection for sterilizing liquids, air, and surfaces. Therefore, a deeper understanding of
45 using UVC to inactivate pathogenic microorganisms might strengthen our ability to address the public health
challenge posed by airborne viruses.

A significant challenge lies in the quantitative determination of the UV radiation dose required to inactivate
pathogenic microorganisms (Gandhi et al., 2012; Feng et al., 2010). Although researchers have investigated the
50 necessary dose of UV radiation to disinfect coronaviruses, it's noteworthy that the calculated and measured UV
dosages in these studies exhibit considerable variations (Walker and Ko, 2007; Buonanno et al., 2020; Tseng and
Li, 2005; Terpstra et al., 2007; Pratelli, 2008; Deshmukh and Pomeroy, 1969; Eickmann et al., 2020; Kariwa et
al., 2006; Kaur and Gupta, 2020). For instance, even within the 254 nm results, the log-reduction doses ranges
widely: it is $0.6 \text{ mW} \cdot \text{s} \cdot \text{cm}^{-2}$ for bovine coronavirus, while for SARS (CoV Urbani), it's as high as $11,754 \text{ mW} \cdot \text{s} \cdot \text{cm}^{-2}$
55 2 (Heßling et al., 2020). The reasons behind this diversity in reported UV doses remain unclear, but possible factors
include differences in culture mediums, experimental facilities, or sample conditions (solid surface, liquid, aerosol)
(Biasin et al., 2021). So far, the inactivation of viral aerosols by UVC radiation has not been as extensively studied
as it has been for liquids and on solid surfaces (Feng et al., 2010; Welch et al., 2018; Hamzavi et al., 2020; Hijnen
et al., 2006; Bohrerova et al., 2005). This is partly due to the high vapor pressure of pure water, which leads to an
60 extremely short evaporation time and consequently unstable aerosol droplets. For example, a pure water droplet
of 100 nm evaporates in approximately two microseconds (Ferron and Soderholm, 1990). This dynamic change in
droplet size can also impact the concentration and susceptibility of airborne microorganisms, presenting a
significant challenge to many medical and biological laboratories studying bioaerosols. Moreover, aerosol experts,
despite their proficiency in aerosol generation and measurement, often encounter difficulties in conducting direct



65 experiments involving pathogenic microorganisms due to the stringent requirement of biosafety laboratory. In this regard, bridging the gap between aerosol scientists and biologists is crucial for a faster and more comprehensive understanding of bioaerosol inactivation using UVC radiation.

70 In various studies, UV-sensitive dyes have been tested as model systems to mimic the behavior of pathogenic microorganisms under UV radiation exposure. For example, the degradation of chromophores and fluorophores has been used to measure the radiation doses of UV light with a wavelength of 254 nm, serving as chemical indicators for UV sterilization processes. The decrease in absorbance or fluorescence has been correlated to the radiation dose in $W \cdot s \cdot cm^{-2}$ and the reduction in the concentration of microorganisms such as *Escherichia coli*, *Staphylococcus aureus*, and *Candida albicans* (Putt et al., 2012). Moreover, UV-sensitive dyes have been utilized
75 to develop colorimetric UV dosimeters that monitor sunlight exposure to prevent skin damage. Wang (Wang et al., 2018) demonstrated a wearable wristband that combined with a colorimetric UV film to indicate the UV dose through the discoloration of a purple photodegradable dye under exposure to UV light. The UV sensing film completely discolors to transparency in two hours under a solar simulator, suggesting its potential as an indicator to help individuals avoid skin damage. Various wearable devices containing UV-sensitive dyes were developed to
80 monitor UV exposure, showing that the degree of sun exposure can be quantified with an accuracy rate of 95% by establishing a correlation between the color changes and the dosage of UVA (400-320 nm) and UVB (315-280 nm) radiation received (Kurz et al., 2020). Nevertheless, all these studies involving UV-sensitive dyes focus on assessing the required UV radiation doses either in liquid solutions or on solid surfaces. When UV-sensitive dyes are aerosolized and exposed to UVC light, it is unclear whether the photodegradation of UV-sensitive dyes linearly
85 increases with the UV radiation dose. Therefore, the use of UV-sensitive dyes in studying UV effects on aerosol droplets could potentially provide valuable insights into UV disinfection mechanisms and their efficacy.

This study presents the development of a model system that enables the determination of the UV radiation dose experienced by an aerosol, without the need for using microorganisms. This model system can generate stable
90 aerosol droplets composed of UV-sensitive dyes and a carrier liquid, di-ethyl-hexyl-sebacate (DEHS). The UV dose received by these aerosol droplets during irradiation can be evaluated by tracking changes in the color intensity of the UV-sensitive dyes. Three critical criteria were established for the selection of UV-sensitive dyes: observable sedimentation, high extinction coefficients in the vicinity of 260 nm, and significant solubility in DEHS. Detailed analysis and discussion were conducted regarding the particle size distribution and number concentration
95 of the aerosol droplets generated from these selected UV-sensitive dye solutions. A low-pressure impactor was developed to collect the aerosolized droplets, thus enabling the assessment of dye content within the aerosol samples. The concentration of the UV-sensitive dye in the collected liquid was then determined using a UV-Vis spectrometer. The feasibility of using UVC light-emitting-diode (LED) irradiation to degrade the UV-sensitive dye solution was also evaluated in this work. The UV dose experienced by the aerosols was determined by passing
100 through a designed UVC irradiation chamber with various residence time. Determination of the UV dose experienced by the aerosols was achieved by irradiating the flowing aerosols in a specifically designed UVC irradiation chamber.

2 Experimental details

2.1 Selection of UV-sensitive dye solutions



105 Due to the dynamic nature of the size of water-based aerosols, DEHS was chosen as the carrier liquid to ensure
the generation of stable droplets with extended lifetimes, allowing for accurate online measurements. The first step
involved selecting a solution containing DEHS and UV-sensitive dyes. 20 types of non-toxic UV-sensitive dyes,
including two water-soluble and 18 fluorescent dyes, were tested for suitability. DEHS (CAS-No.: 122-62-3),
Erythrosin B (CAS-No.: 568-63-8), and Indigo Carmine (CAS-No.: 865-22-0) were procured from the Merck
110 Group (Sigma-Aldrich Chemie GmbH, Taufkirchen, Germany), while a fluorescent dye kit (Part Number: DFKIT-
COMP) was purchased from the Risk Reactor Inc. (California, United States of America). Detailed information
about all the tested UV-sensitive dyes is provided in table 1. Initially, solutions containing DEHS and UV-sensitive
dyes were prepared at a concentration of $100 \mu\text{g}\cdot\text{mL}^{-1}$ and left undisturbed for 48 hours. Eight of these solutions,
which demonstrated no noticeable sedimentation, were selected for further evaluation. The UV-Vis absorbance
115 spectra of these eight dye solutions were then determined using an ultraviolet-visible (UV-Vis) spectrophotometer
(Cary 500 UV-Vis-NIR Spectrophotometer, Agilent Technologies, USA). Given the varying susceptibility of
different UV-sensitive dyes to UVC exposure, those with UVC susceptibility similar to deoxyribonucleic acid
(DNA) or ribonucleic acid (RNA) were identified for further investigation. In the third stage, the relationship
between absorbance and concentration of the dye solutions was analyzed to quantitatively assess their solubility
120 in DEHS. The selected dyes were prepared at concentrations of $20 \mu\text{g}\cdot\text{mL}^{-1}$, $15 \mu\text{g}\cdot\text{mL}^{-1}$, $10 \mu\text{g}\cdot\text{mL}^{-1}$, $5 \mu\text{g}\cdot\text{mL}^{-1}$,
and $1 \mu\text{g}\cdot\text{mL}^{-1}$, after which their UV-Vis absorbance spectra were measured from 260 nm to 800 nm at two nm
intervals. The maximum peak absorbance in the visible region was identified for each dye. All solutions were
prepared with highly accurate graduated pipettes and an analytical balance (XS205, Mettler-Toledo AG,
Switzerland). To ensure an accurate representation of the average absorbance values, all concentrations were
125 prepared in triplicate.

Table 1: Summarized information on all the tested UV-sensitive dyes.

Sample No.	Dye Info.	Manufacturer
#1	Erythrosine B	Sigma-Aldrich
#2	Indigo Carmine	Sigma-Aldrich
#3	DFSB-K427	Risk Reactor Inc.
#4	DFSB-K400	Risk Reactor Inc.
#5	DFSB-K87	Risk Reactor Inc.
#6	DFSB-K41-50	Risk Reactor Inc.
#7	DFSB-K44-65	Risk Reactor Inc.
#8	DFSB-K52	Risk Reactor Inc.
#9	DFSB-K160	Risk Reactor Inc.
#10	DFSB-K401	Risk Reactor Inc.
#11	DFSB-K413	Risk Reactor Inc.
#12	DFWB-K1-60	Risk Reactor Inc.
#13	DFWB-K7	Risk Reactor Inc.
#14	DFSB-K149	Risk Reactor Inc.
#15	DFWB-K250	Risk Reactor Inc.
#16	TACID9501	Risk Reactor Inc.
#17	DFSB-K184	Risk Reactor Inc.
#18	DFSB-K40 & DFWB-K40	Risk Reactor Inc.
#19	DFSB-K52-55	Risk Reactor Inc.
#20	DFWB-K73-51	Risk Reactor Inc.

2.2 Experimental setup for investigation of aerosols containing UV-sensitive dyes

2.2.1 Low-pressure impactor for aerosol droplet collection



140 To evaluate the concentration changes of dye-laden aerosols, a one-stage low-pressure impactor (LPI) was developed for collecting aerosol droplets both before and after UV irradiation treatment. Under the assumption of no evaporation and complete collection of all aerosol particles, the concentration inside the aerosol droplets should remain unchanged. The LPI design was based on the geometry of an electrostatic precipitator developed at the institute of technology for nanostructures (NST, University of Duisburg-Essen, Duisburg, Germany), as illustrated in Fig. 1. The inlet gas flow could be controlled via different critical orifices to adjust the desired residence time in the UV irradiation zone. The outlet of the LPI was connected to a rotary vane pump (Type 301853, ILMVAC GmbH, Ilmenau, Germany), maintaining the measured pressure inside the impactor chamber at less than 0.22 bar. As shown in Fig. 1, the distance between the collecting substrate and the aerosol outlet z was 5 mm. The collection efficiency of the LPI was determined by comparing the aerosol droplets mass concentration, as obtained by a tapered element oscillating microbalance (TEOM; Model 1405, Thermo Fisher Scientific, Waltham, USA), to the collected liquid mass, under defined aerosol flow and collection time. The impact of sampling using the lab-built impactor on the UV-Vis spectra of UV-sensitive dyes (#4 and #7 in Table 1) was also investigated. UV-sensitive dye solutions at various concentrations ($20 \mu\text{g}\cdot\text{mL}^{-1}$, $15 \mu\text{g}\cdot\text{mL}^{-1}$, $10 \mu\text{g}\cdot\text{mL}^{-1}$, $5 \mu\text{g}\cdot\text{mL}^{-1}$ and $1 \mu\text{g}\cdot\text{mL}^{-1}$) were applied to generate aerosols using a commercial aerosol droplet generator (AGF 2.0, Palas GmbH, Germany). Droplets of each concentration were collected over a two-hour period using the lab-built impactor, equipped with a 1 mm critical orifice (gas flow $8.8 \text{ L}\cdot\text{min}^{-1}$). The collected liquids were transferred to a quartz submicron cuvette (Part number: 6610024100, Agilent Technologies, Santa Clara, USA), having a minimum capacity of $80 \mu\text{L}$, for UV-Vis spectra measurements. The corresponding concentration of dye solutions was determined using the previously mentioned UV-Vis spectrophotometer.

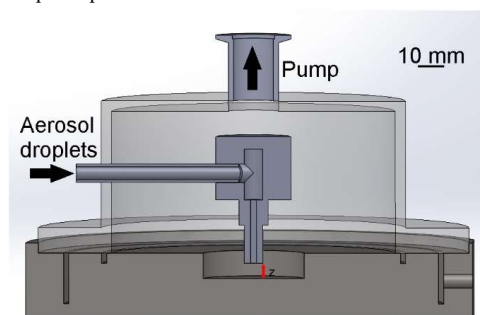


Figure 1: Schematic of the designed low-pressure impactor for aerosol collection in this study.

2.2.2 UV irradiation of UV-sensitive dyes

160 Before constructing the UV irradiation chamber, a UVC LED module with a wavelength of 275 nm (part number: 37337, Lumitronix LED-Technik GmbH, Hechingen, Germany) was employed to assess whether the selected dyes would degrade upon UV irradiation. As depicted in Fig. 2, one milliliter of the dye solutions was added to the aforementioned cuvette used for measuring collected aerosol droplets. A specially designed 3D-printed fixture held the quartz cuvette in a fixed position as it underwent irradiation for various durations. A UV light meter (UV-integrator Typ D, Beltron GmbH, Roedermark, Germany) was used to measure the radiation intensity ($\text{mW}\cdot\text{cm}^{-2}$) at the same position. The UV radiation dose ($\text{mW}\cdot\text{s}\cdot\text{cm}^{-2}$) was calculated by multiplying the measured intensity ($\text{mW}\cdot\text{cm}^{-2}$) by the irradiation duration (seconds). The UV-Vis absorbance spectra of the dye solutions were recorded both before and after irradiation.

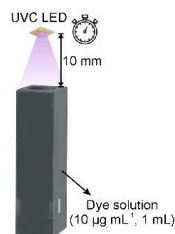


Figure 2: Experimental apparatus used to study the dye solution degradation upon UVC irradiation.

170 Figure 3 shows a schematic overview of the aerosol irradiation chamber. The constructed chamber comprises a quartz tube, a UVC LED array, and 3D printed fixtures. The UVC LED array (Part number: ILS-XN12-S260-0280-SC201-W2, Intelligent LED Solutions, Berkshire, United Kingdom) consists of 12 UVC LEDs (with a radiation peak at 270 nm) that are connected and arrayed linearly to electronic printed circuit boards (PCB). A heat sink and two cooling fans were implemented to enhance the performance of the UV LEDs by dissipating heat from the PCB. In this setup, the UVC LED array was positioned with its surface parallel to the bottom of the quartz tube, at a one-centimeter distance. The UV light traveled through the quartz tube and irradiated the flowing aerosols within the chamber. The intensity of the UV radiation is adjustable by modulating the current of the UVC LED array (300–1050 mA). A radiometer, equipped with a UV-3726-5 detector (X1-5, Gigahertz Optik GmbH, Tuekenfeld, Germany) and calibrated with a 260–290 nm LED, was applied for the measurement of the UVC radiation intensity. To assess the average radiation intensity inside the chamber, a detector fixture was designed to position the detector surface at half the height of the chamber. The UV intensity experienced by an aerosol droplet was then determined by averaging the measured intensities at five different spots. The exposure time t of the aerosol to the UV radiation is approximated by the mean residence time of the aerosol in the device, defined as $t = V/q$, with V the effective irradiation volume of the quartz tube (777 cm^3) and q the aerosol flow rate. Table 2 summarizes the specifications of the UV chamber and the calculated UV dose used in this study.

Table 2: Specifications of the UV irradiation chamber applied in this study to irradiate aerosols.

UV irradiation chamber with various dose settings			
Critical orifice	0.3 mm	0.5 mm	1.0 mm
Calibrated gas flow	$0.78 \text{ L} \cdot \text{min}^{-1}$	$2.26 \text{ L} \cdot \text{min}^{-1}$	$8.86 \text{ L} \cdot \text{min}^{-1}$
Chamber irradiation length	275 mm	275 mm	275 mm
Chamber internal diameter	600 mm	600 mm	600 mm
Exposure time	59.8 s	20.6 s	5.3 s
UVC LED current	1000 mA	1000 mA	1000 mA
Calibrated intensity	$4.10 \text{ mW} \cdot \text{cm}^{-2}$	$4.10 \text{ mW} \cdot \text{cm}^{-2}$	$4.10 \text{ mW} \cdot \text{cm}^{-2}$
UV radiation dose	$245.1 \text{ mW} \cdot \text{s} \cdot \text{cm}^{-2}$	$84.6 \text{ mW} \cdot \text{s} \cdot \text{cm}^{-2}$	$21.6 \text{ mW} \cdot \text{s} \cdot \text{cm}^{-2}$

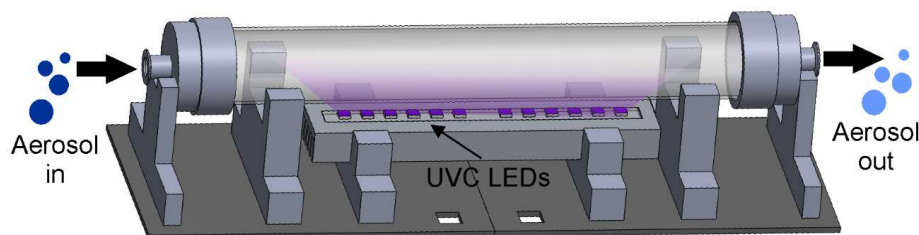


Figure 3: Schematic overview of the constructed UV irradiation chamber.



2.2.3 Characterization of aerosol droplets containing UV-sensitive dyes

Figure 4 presents the schematic of the overall experimental setup for studying aerosol droplets containing UV-sensitive dyes. Briefly, a liquid nebulizer featuring a two-substance nozzle and a cyclone ($d_{p, max} = 2 \mu\text{m}$) was used to generate aerosols from the selected UV-sensitive dye solutions. The aerosol particle size distribution and concentration, both before and after passing through the designed UV irradiator, were investigated using online measurements. This study applied conventional aerosol measurement devices, including a scanning mobility particle sizer (SMPS; Model 3938, TSI, Minneapolis, USA), an electrical low-pressure impactor (ELPI; Model ELPI+, Dekati Ltd., Tampere, Finland), and a tapered element oscillating microbalance (TEOM). An aerosol dilution system with a dilution ratio of 100 (VKL10 + VKL10 cascade system, Palas GmbH, Karlsruhe, Germany) was utilized to lower the particle number concentration for the standard online instruments. This dilution technique did not significantly alter the particle size distribution. The above-mentioned low-pressure impactor was employed to collect aerosols before and after passing through the designed UV irradiation chamber, to characterize how the selected dyes would degrade upon UV irradiation. A UV-Vis spectrophotometer was used to determine the changes in dye concentration of the collected liquids before and after UV irradiation.

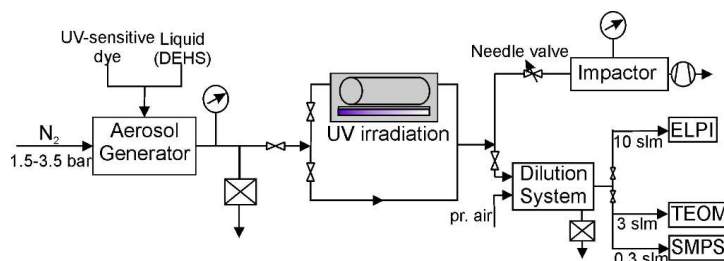


Figure 4: Experimental setup to investigate the effect of UV irradiation on the concentration of aerosol droplets before and after irradiation.

3 Results and discussion

3.1 Generation of an aerosol containing UV-sensitive dyes

3.1.1 Selection of UV-sensitive dyes with high solubility in DEHS (three criteria)

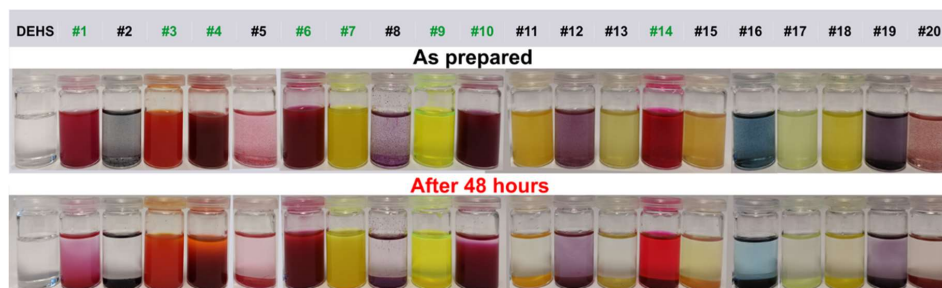
As noted earlier, due to the rigorous requirements of biosafety laboratories, many aerosol laboratories are often unable to conduct experiments with pathogenic microorganisms. In this study, DEHS was chosen as the carrier liquid for generating non-biological and stable aerosol droplets. Consequently, a key criterion for selecting suitable UV-sensitive dyes was their high solubility in DEHS. Solubility can range from infinite to virtually insoluble, and the threshold value definition varies depending on the application. To rapidly screen UV-sensitive dyes soluble in DEHS, solutions were prepared at a dye concentration of $100 \mu\text{g}\cdot\text{mL}^{-1}$. These solutions were then left undisturbed for 48 hours, during which the sedimentation process was recorded, as demonstrated in Fig. 5. From these visual observations, eight solutions with no significant sedimentation were chosen for the next step: dyes #1, #3, #4, #6, #7, #9, #10, and #14. An overview of all measurements conducted for the selection of UV-sensitive dyes is provided in Table 3.



215 **Table 3: Comprehensive overview of measurements conducted for UV-sensitive dye selection.**

Sample No.	Step 1 Sedimentation	Step 2 UV-Vis absorbance	Step 3 Linear relationship
#1	✓	✓	×
#2	✓	×	×
#3	✓	✓	✓
#4	✓	✓	✓
#5	✓	×	×
#6	✓	✓	✓
#7	✓	✓	✓
#8	✓	×	×
#9	✓	✓	×
#10	✓	✓	×
#11	✓	×	×
#12	✓	×	×
#13	✓	×	×
#14	✓	✓	×
#15	✓	×	×
#16	✓	×	×
#17	✓	×	×
#18	✓	×	×
#19	✓	×	×
#20	✓	×	×

220 The ultraviolet light spectrum theoretically ranges from 100 to 480 nm and is divided into four regions: UVA (320-400 nm), UVB (290-320 nm), UVC (200-290 nm), and VUV (100-200 nm). UVC radiation is the most potent for pathogen inactivation as the maximum absorbance of DNA and RNA occurs around 260 nm (Mankar et al., 2022). Consequently, another key criterion for selecting a UV-sensitive dye is its high absorption capacity around 260 nm. For this consideration, the UV-Vis absorbance spectra of all eight dye solutions were measured. It should be mentioned that pure DEHS liquid was used as the baseline, and all spectra were derived by subtraction this baseline. The similarity of these spectra led to their division into three groups. As detailed in Fig. 6, it can be observed that two of the tested dyes (categorized as Group A) might undergo chemical reactions or polarization with DEHS liquid, as indicated by broad absorption peaks. Sharp absorption peaks in UV-Vis spectroscopy are desired in this study to quantitatively evaluate concentration changes after UV irradiation. Thus, the Group A dyes were deemed unsuitable for further investigation. In contrast, the two dyes categorized as Group B displayed sharp absorption peaks in the visible region. For comparison, all spectra were normalized at the wavelength where maximal absorption peak occurs. However, these Group B dyes failed to show significant absorption characteristics near the desired 260 nm range, leading to their exclusion from subsequent studies. Only four dyes, assigned to Group C, fulfilled this criterion. These dyes displayed distinct absorption characteristics near 260 nm and sharp absorption peaks in the visible region.



230 **Figure 5: Sedimentation observation of 20 various dye solutions.**



To ensure a homogeneous dye distribution within the aerosol droplet, it is essential to have a high dissolution rate for the selected dye in the DEHS solvent. The correlation between the absorbance and the concentration of the dye solutions was examined to quantitatively evaluate the solubility level of the chosen dyes (#3, #4, #6, #7 in Tab. 1).
 235 Figure 7 presents the typical UV absorption spectra of an unsuitable dye (#3) and a suitable dye (#4) with concentration ranging from $1 \mu\text{g}\cdot\text{mL}^{-1}$ to $20 \mu\text{g}\cdot\text{mL}^{-1}$. A linear fit was established for each dye based on the maximum absorbance in the visible spectrum region. The results revealed that two of the tested dyes (#4 and #7) had a goodness of fit (R-squared) value greater than 0.99 in a simple linear regression, suggesting superior dissolution and long-term stability in DEHS. As a result, these two dyes (#4 and #7) with higher linearity were
 240 selected as candidates for the model system in this research study, as dye degradation was used to quantify the UV radiation dose.

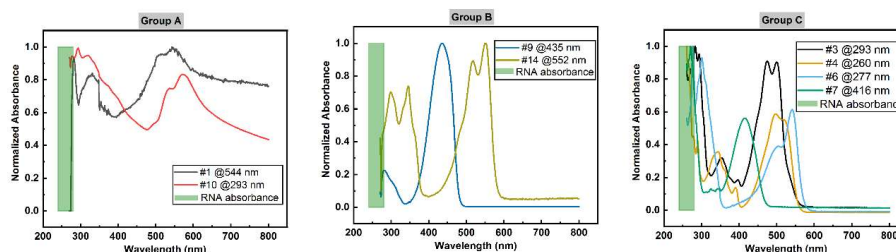


Figure 6: UV-Vis Spectra of dye solutions, where only group C is suitable due to their absorption characteristic in the vicinity of 260 nm and in the visible region.

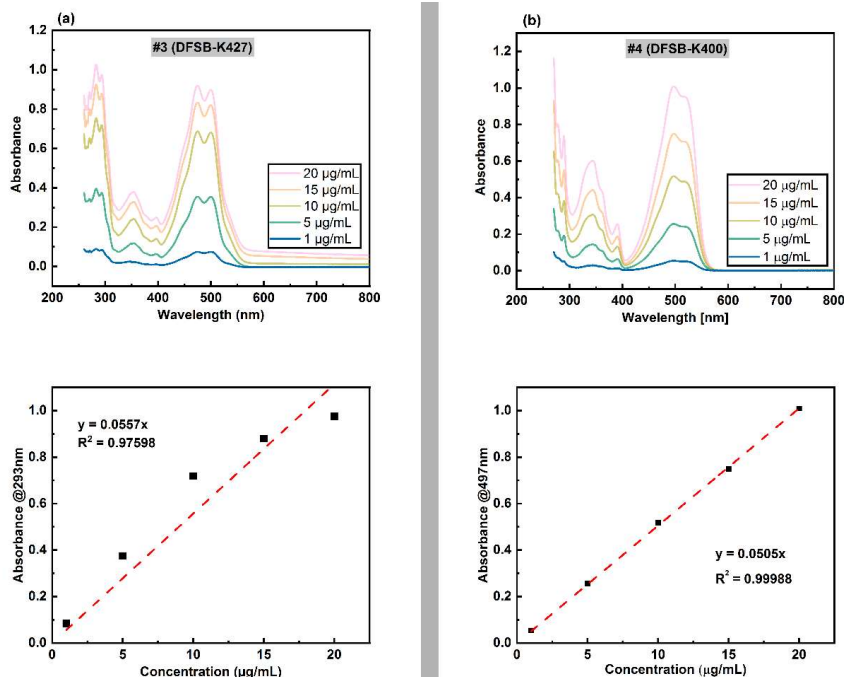


Figure 7: UV-Vis spectra with various concentrations (top) and the corresponding standard curve for dye solutions (bottom), where #3 (left) is the typical example of unsuitable dye and #4 (right) is an example of suitable dye.



3.1.2 Effect of the addition of UV-sensitive dyes on the particle size distribution

Our main objective was to develop a stable dye-laden aerosol model to estimate the UV radiation dose experienced by an aerosol droplet. Previous research has suggested that most exhaled aerosol droplets are smaller than 5 μm , including aerosols produced by breathing, speaking, and coughing. More recent studies have shown that aerosols smaller than 1 μm pose significant concern regarding disease transmission since these smaller particles remain in the air longer and can deposit in the respiratory tract to initiate infection (Wang et al., 2018). Therefore, this study on determining the UVC radiation dose required for aerosols primarily focused on evaluating smaller particle-sized aerosols. A commercial aerosol generator was employed to atomize DEHS liquid, where the carrier gas flow is adjustable by setting the operation pressure of compressed nitrogen. The aerosol generator was equipped with a cyclone ($d_{p, \text{max}} = 2 \mu\text{m}$) so that aerosols larger than 2 μm would not leave the generator. Figure 8 shows the particle size distribution, based on the mobility equivalent diameter measured by SMPS and the Stokes diameter measured by ELPI, of DEHS aerosols produced at various operating pressures of the aerosol generator. It is evident that an increase in the operating pressure correspondingly increased the particle number concentration, while the particle size distribution remained relatively unchanged. The generated aerosol droplets exhibited a size distribution similar to that of most respiratory droplets, with a large fraction is smaller than 1 μm and a peak around 0.2 to 0.8 μm (Morawska et al., 2009; Zayas et al., 2012; Fabian et al., 2011). Furthermore, the particle number concentration of the DEHS droplets produced at a pressure of 2.0 bar aligns closely with the concentration of the cough-generated droplets (Zayas et al., 2012). For these reasons, a pressure of 2.0 bar was chosen to produce DEHS aerosols in subsequent studies.

In addition, the influence of adding UV-sensitive dye on the particle size distribution of DEHS aerosols was investigated. The previously selected dyes, either #4 or #7, were dispersed in DEHS liquid to prepare dye solutions with a concentration of 10 $\mu\text{g}\cdot\text{mL}^{-1}$, respectively. These prepared dye solutions were fed into the aerosol generator, which was subsequently driven by a pressure of 2.0 bar to generate droplets containing UV-sensitive dyes. Figure 9 displays the particle size distribution and number concentration of the generated dye-laden droplets as well as pure DEHS droplets. All measurements, including aerosol generation and online characterization, were conducted continuously over a one-hour period. Based on these experimental observations, the slight fluctuation in the number concentration is likely due to the instability of the aerosol generator. Therefore, it can be concluded that the addition of UV-sensitive dyes (at 10 $\mu\text{g}\cdot\text{mL}^{-1}$) does not significantly affect the particle size and number concentration of DEHS aerosols.

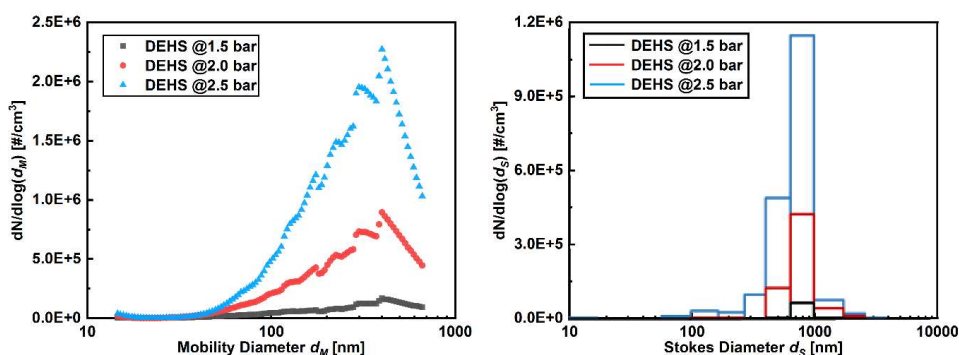


Figure 8: Particle size distribution of DEHS aerosols at various operating pressures of the aerosol generator.

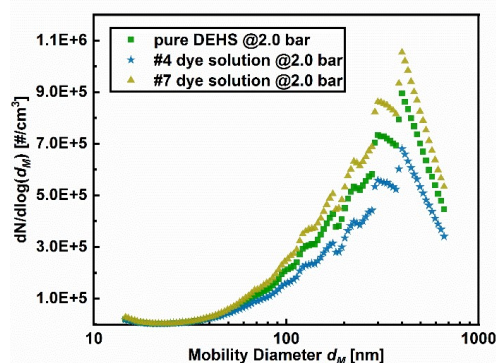


Figure 9: Comparison of particle size distribution (measured by SMPS) of aerosols generated from dye solutions and pure DEHS, respectively.

3.2 Effect of impactor sampling on dye content in aerosols

275 Sampling airborne pathogens poses significant challenges as most bioaerosols are water-based, and their particle size can change due to evaporation during the sampling process. In this study, DEHS, an oily liquid, was chosen to generate aerosols, eliminating the complexity associated with liquid evaporation. A lab-built impactor was designed to collect dye-containing droplets before and after their passage through a UV irradiation chamber. The aerosol mass concentration was directly measured online using a TEOM to estimate the collection efficiency. Concurrently, aerosol droplets were collected using the impactor at a defined aerosol flow rate ($8.8 \text{ L} \cdot \text{min}^{-1}$) for one hour. Dye solutions with concentrations ranging from $1 \mu\text{g} \cdot \text{mL}^{-1}$ to $20 \mu\text{g} \cdot \text{mL}^{-1}$ were utilized for these measurements. The collection efficiency was determined to be above 90% by comparing the mass output of the aerosol generator to the collected liquid. Moreover, the absorbance of all collected liquids was measured to compare the concentration with those in the liquid reservoir of the aerosol generator, as demonstrated in Fig. 10.

280

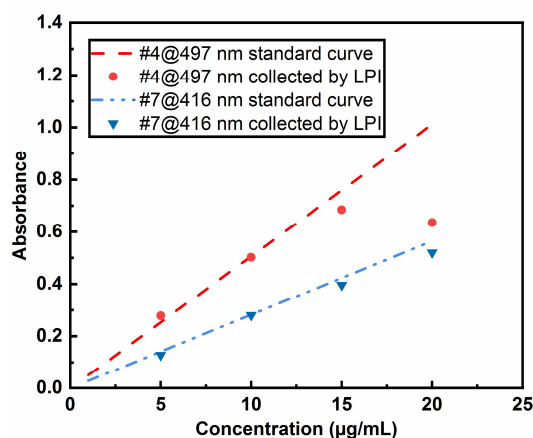


Figure 10: Effect of LPI collection on the dye concentrations by using various concentrations of dye solutions.

Notably, concentration deviations became increasingly pronounced when higher concentrations of dye solutions ($> 15 \mu\text{g} \cdot \text{mL}^{-1}$) were used to generate aerosols. This observation could potentially be explained by the dependence of the dye concentration in a droplet on the size of the droplet. Both the measured and theoretically calculated results revealed that the maximal collection volume of DEHS droplets, using the aerosol generator AGF 2.0 at a

285



pressure of 1.5 bar, was at $96 \mu\text{L}\cdot\text{h}^{-1}$. In the current study, a one-stage impactor was developed to capture the generated polydisperse droplets for UV-Vis spectrum analysis, which expedited the collection process and efficiency. However, this approach did not consider the potential influence of droplet size on the dye concentration and degradation. Future studies should generate or classify narrower aerosol fractions instead of a broad aerosol distribution to investigate potential particle size effects. To mitigate the effect of dye concentration deviation, a concentration of $10 \mu\text{g}\cdot\text{mL}^{-1}$ was employed, ensuring that each dye (#4, #7) remained well within the linear range for the UVC degradation studies.

3.3 Determination of dye degradation of selected UV-sensitive dyes

295 Currently, most UV disinfection systems for water, air, and surfaces continue to utilize conventional low- or medium-pressure mercury lamps. The primary concern with these lamps is their fragility and their containment of toxic mercury, which poses environmental hazards and requires proper disposal. UV LEDs, on the other hand, are emerging as a popular, environmentally friendly alternative. Their compact size simplifies their integration into sterilization systems, and they offer a diverse range of wavelengths (Kim and Kang, 2018; Song et al., 2016).
300 Considering the above reasons, this study employed UVC LEDs to investigate dye degradation upon UV radiation. To characterize the degradation of the selected UV-sensitive dyes upon UV irradiation, 1 ml of a $10 \mu\text{g}\cdot\text{mL}^{-1}$ dye solution was added to a quartz cuvette. Figure 11 presents the measured UV-Vis spectra of dye solutions before and after irradiation with various UV radiation doses. As the UV radiation dose increased, the maximal absorbance values in the visible region decreased noticeably. Moreover, despite a similar degradation trend observed for the two tested dye solutions, dye solution #4 demonstrated a higher sensitivity to UVC irradiation at 275 nm. It is worth noting a prior study that used the degradation of water-based dye solutions to measure UV dose. This study irradiated a dye solution on (1 ml and $10 \mu\text{g}\cdot\text{mL}^{-1}$) in a quartz cuvette with 254 nm UV light. It was observed that the required UV dosage for the degradation of dye #4 (497 nm) and dye #7 (419 nm) aligns with the order of magnitude specified for Fast Green (624 nm), Allura Red (495 nm), and Tartrazine (426 nm) by the study
305 conducted by Putt (Putt et al., 2012).
310

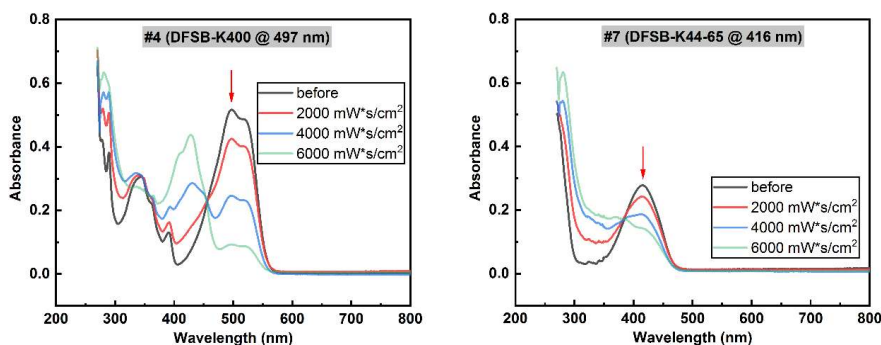


Figure 11: Dye solution degradation upon UV irradiation using a UVC LED (275 nm).

Based on prior research indicating that dye #4 displayed heightened sensitivity to UVC radiation, this dye solution was chosen for aerosol droplet generation. The UV dose received by the droplets was estimated by multiplying the UV intensity by the average residence time of aerosols inside the exposure chamber. In the current study, the UV radiation dose was modulated by controlling the carrier gas flow rate, where the applied current of the UVC



315 LED array was maintained to 1000 mA. The estimated UV radiation doses were $245.1 \text{ mW}\cdot\text{s}\cdot\text{cm}^{-2}$ at $0.78 \text{ l}\cdot\text{min}^{-1}$,
 $84.6 \text{ mW}\cdot\text{s}\cdot\text{cm}^{-2}$ at $2.26 \text{ l}\cdot\text{min}^{-1}$, and $21.6 \text{ mW}\cdot\text{s}\cdot\text{cm}^{-2}$ at $8.86 \text{ l}\cdot\text{min}^{-1}$, respectively. The influence of UV dose on
the degradation of dye-laden aerosols can be demonstrated in Fig. 12. When exposed to a 270 nm UVC array at a
dose of $245.1 \text{ mW}\cdot\text{s}\cdot\text{cm}^{-2}$, an approximate 10% degradation of the dyes within the aerosols sampled was noted.
320 Meanwhile, a lower UV dose of $21.6 \text{ mW}\cdot\text{s}\cdot\text{cm}^{-2}$ was capable of degrading 5% of the dye-containing aerosol
droplets. These results suggest a non-linear relationship between the survival of UV-sensitive dyes and the increase
in UV radiation doses. It's worth noting that increasing the UV dose by extending droplet residence time in the
exposure section is not ideal. Observations revealed that a longer residence time resulted in droplets deposition on
the quartz tube wall. This occurrence reduces the collection efficiency by the low-pressure impactor and diminishes
the UV radiation intensity entering the chamber. Therefore, it is recommended to adjust the UV dose by altering
325 the power of UVC LEDs and limiting the residence time of aerosol droplets.

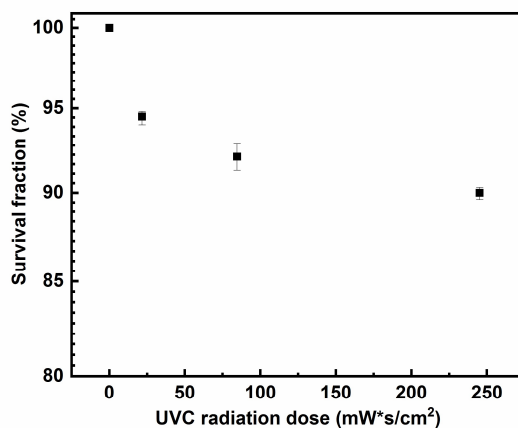


Figure 12: Effect of UVC radiation dose on the dye survival within aerosol droplets.



4 Conclusions

It is known that aerosolized viruses can effectively be disinfected by the use of UVC radiation, where its effectiveness depends on the UV dose experienced by the aerosol. The dose required for disinfection can be determined on immobilized viruses in biosafety laboratories, whereas determining the dose experienced by an aerosol in a given UV disinfection apparatus or a room equipped with UV disinfection can conveniently be done with the help of suitable nonbiogenic aerosols. Here, this study proposes a model system consisting of nonevaporating DEHS droplets containing a UV-sensitive dye. From an initial selection of 20 UV-sensitive dyes, only two were deemed suitable based on key selection criteria: prominent absorption characteristics around 260 nm and high solubility in DEHS. Moreover, it has been demonstrated that adding UV-sensitive dyes ($10 \mu\text{g}\cdot\text{mL}^{-1}$) did not affect the particle size and number concentration of DEHS-based aerosols. For analyzing the concentration changes before and after passing through a UV irradiation chamber, a low-pressure impactor was designed to collect dye-containing aerosol droplets and transfer the liquid into a quartz cuvette. The potential of using UVC LED irradiation to degrade the UV-sensitive dye solution was also examined, leading to the development of a UV radiation chamber capable of modulating the UV dose. The self-built UVC irradiation chamber allows for the quantitative determination of the UV dose experienced by aerosols with UV-sensitive dyes. The obtained results indicate a non-linear correlation between the survival rate of UV-sensitive dyes and the increase in UV radiation doses. Specifically, a UVC dose of $245.1 \text{ mW}\cdot\text{s}\cdot\text{cm}^{-2}$ at 270 nm degraded approximately 10% of the dyes in DEHS aerosols, while a lower dose of $21.6 \text{ mW}\cdot\text{s}\cdot\text{cm}^{-2}$ degraded 5% of the dye-laden aerosols. In summary, our study demonstrated the feasibility of quantitatively determining the UV radiation dose experienced by an aerosol droplet by incorporating UV-sensitive dyes into droplets. Further research is necessary to understand the impact of the suspending medium and the aerosol droplet size on the required UV dose for dye degradation.

350 CRediT authorship contribution statement

Frank Einar Kruis: Supervision, Funding acquisition, conceptualization, review & editing. **Qingqing Fu:** Conceptualization, Investigation, Visualization, Writing – original draft preparation. All authors have read and agreed to the published version of the manuscript.

355 Declaration of competing interest

The authors declare that they have no known competing financial interests or personal relationships that could have appeared to influence the work reported in this paper.

Acknowledgement

360 We would like to thank “Deutsche Forschungsgemeinschaft” (DFG) for financially supporting this research project (grant no. 469047872).



References

- Abkar, L., Zimmermann, K., Dixit, F., Kheyrandish, A., and Mohseni, M.: COVID-19 pandemic lesson learned-critical parameters and research needs for UVC inactivation of viral aerosols, *Journal of Hazardous Materials Advances*, 8, 100183, <https://doi.org/10.1016/j.hazadv.2022.100183>, 2022.
- 365 Biasin, M., Bianco, A., Pareschi, G., Cavalleri, A., Cavatorta, C., Fenizia, C., Galli, P., Lessio, L., Lualdi, M., Tombetti, E., Ambrosi, A., Redaelli, E. M. A., Saulle, I., Trabattoni, D., Zanutta, A., and Clerici, M.: UV-C irradiation is highly effective in inactivating SARS-CoV-2 replication, *Sci Rep*, 11, 6260, <https://doi.org/10.1038/s41598-021-85425-w>, 2021.
- 370 Bohrerova, Z., Bohrer, G., Mohanraj, S. M., Ducoste, J., and Linden, K. G.: Experimental Measurements of Fluence Distribution in a UV Reactor Using Fluorescent Microspheres, *Environ. Sci. Technol.*, 39, 8925–8930, <https://doi.org/10.1021/es050034c>, 2005.
- Buonanno, M., Welch, D., Shuryak, I., and Brenner, D. J.: Far-UVC light (222 nm) efficiently and safely inactivates airborne human coronaviruses, *Sci Rep*, 10, 10285, <https://doi.org/10.1038/s41598-020-67211-2>, 2020.
- 375 Deshmukh, D. R. and Pomeroy, B. S.: Ultraviolet Inactivation and Photoreactivation of Avian Viruses, *Avian Diseases*, 13, 596, <https://doi.org/10.2307/1588533>, 1969.
- Dong, E., Du, H., and Gardner, L.: An interactive web-based dashboard to track COVID-19 in real time, *The Lancet Infectious Diseases*, 20, 533–534, [https://doi.org/10.1016/S1473-3099\(20\)30120-1](https://doi.org/10.1016/S1473-3099(20)30120-1), 2020.
- 380 Eickmann, M., Gravemann, U., Handke, W., Tolksdorf, F., Reichenberg, S., Müller, T. H., and Seltsam, A.: Inactivation of three emerging viruses – severe acute respiratory syndrome coronavirus, Crimean–Congo haemorrhagic fever virus and Nipah virus – in platelet concentrates by ultraviolet C light and in plasma by methylene blue plus visible light, *Vox Sang*, 115, 146–151, <https://doi.org/10.1111/vox.12888>, 2020.
- Fabian, P., Brain, J., Houseman, E. A., Gern, J., and Milton, D. K.: Origin of Exhaled Breath Particles from Healthy and Human Rhinovirus-Infected Subjects, *Journal of Aerosol Medicine and Pulmonary Drug Delivery*, 24, 137–147, <https://doi.org/10.1089/jamp.2010.0815>, 2011.
- 385 Feng, Y., Smith, D. W., and Bolton, J. R.: A Potential New Method for Determination of the Fluence (UV Dose) Delivered in UV Reactors Involving the Photodegradation of Free Chlorine, *Water Environment Research*, 82, 328–334, <https://doi.org/10.2175/106143009X447920>, 2010.
- Ferron, G. A. and Soderholm, S. C.: Estimation of the times for evaporation of pure water droplets and for stabilization of salt solution particles, *Journal of Aerosol Science*, 21, 415–429, [https://doi.org/10.1016/0021-8502\(90\)90070-E](https://doi.org/10.1016/0021-8502(90)90070-E), 1990.
- 390 Gandhi, V. N., Roberts, P. J. W., and Kim, J.-H.: Visualizing and Quantifying Dose Distribution in a UV Reactor Using Three-Dimensional Laser-Induced Fluorescence, *Environ. Sci. Technol.*, 46, 13220–13226, <https://doi.org/10.1021/es303133f>, 2012.
- 395 Hamzavi, I. H., Lyons, A. B., Kohli, I., Narla, S., Parks-Miller, A., Gelfand, J. M., Lim, H. W., and Ozog, D. M.: Ultraviolet germicidal irradiation: Possible method for respirator disinfection to facilitate reuse during the COVID-19 pandemic, *Journal of the American Academy of Dermatology*, 82, 1511–1512, <https://doi.org/10.1016/j.jaad.2020.03.085>, 2020.
- 400 Heßling, M., Hönes, K., Vatter, P., and Lingenfelder, C.: Ultraviolet irradiation doses for coronavirus inactivation – review and analysis of coronavirus photoinactivation studies, *GMS Hygiene and Infection Control*; 15:Doc08, <https://doi.org/10.3205/DGKH000343>, 2020.
- Hijnen, W. A. M., Beerendonk, E. F., and Medema, G. J.: Inactivation credit of UV radiation for viruses, bacteria and protozoan (oo)cysts in water: A review, *Water Research*, 40, 3–22, <https://doi.org/10.1016/j.watres.2005.10.030>, 2006.
- 405 Inagaki, H., Saito, A., Sugiyama, H., Okabayashi, T., and Fujimoto, S.: Rapid inactivation of SARS-CoV-2 with deep-UV LED irradiation, *Emerging Microbes & Infections*, 9, 1744–1747, <https://doi.org/10.1080/22221751.2020.1796529>, 2020.
- 410 Kariwa, H., Fujii, N., and Takashima, I.: Inactivation of SARS Coronavirus by Means of Povidone-Iodine, *Physical Conditions and Chemical Reagents, Dermatology*, 212, 119–123, <https://doi.org/10.1159/000089211>, 2006.



- Kaur, S. P. and Gupta, V.: COVID-19 Vaccine: A comprehensive status report, *Virus Research*, 288, 198114, <https://doi.org/10.1016/j.virusres.2020.198114>, 2020.
- Kim, D.-K. and Kang, D.-H.: UVC LED Irradiation Effectively Inactivates Aerosolized Viruses, Bacteria, and Fungi in a Chamber-Type Air Disinfection System, *Appl Environ Microbiol.*, 84, e00944-18, <https://doi.org/10.1128/AEM.00944-18>, 2018.
- 415 Kurz, W., Yetisen, A. K., Kaito, M. V., Fuchter, M. J., Jakobi, M., Elsner, M., and Koch, A. W.: UV-Sensitive Wearable Devices for Colorimetric Monitoring of UV Exposure, *Adv. Optical Mater.*, 8, 1901969, <https://doi.org/10.1002/adom.201901969>, 2020.
- 420 Lefebvre, X., Succar, A., Bédard, E., Prévost, M., and Robert, E.: Characterization of drying bioaerosols with four size distribution measurement instruments in the context of airborne transmission, *In Review*, <https://doi.org/10.21203/rs.3.rs-2207576/v1>, 2022.
- Leung, W. W. F. and Sun, Q.: Electrostatic charged nanofiber filter for filtering airborne novel coronavirus (COVID-19) and nano-aerosols, *Separation and Purification Technology*, 250, 116886, <https://doi.org/10.1016/j.seppur.2020.116886>, 2020.
- 425 Mankar, V., Dhengre, A., Agashe, N., Rodge, H., and Chandi, D. H.: Ultraviolet irradiation doses for coronavirus inactivation -review and analysis of coronavirus photo inactivation studies, *ijhs*, 466–472, <https://doi.org/10.53730/ijhs.v6nS2.5038>, 2022.
- Morawska, L., Johnson, G. R., Ristovski, Z. D., Hargreaves, M., Mengersen, K., Corbett, S., Chao, C. Y. H., Li, Y., and Katoshevski, D.: Size distribution and sites of origin of droplets expelled from the human respiratory tract during expiratory activities, *Journal of Aerosol Science*, 40, 256–269, <https://doi.org/10.1016/j.jaerosci.2008.11.002>, 2009.
- 430 Muñoz, M., Comtois-Bona, M., Cortes, D., Cimenci, C. E., Du, Q., Thompson, C., Figueroa, J. D., Franklin, V., Liu, P., and Alarcon, E. I.: Integrated photothermal decontamination device for N95 respirators, *Sci Rep*, 11, 1822, <https://doi.org/10.1038/s41598-020-80908-8>, 2021.
- 435 Pratelli, A.: Canine coronavirus inactivation with physical and chemical agents, *The Veterinary Journal*, 177, 71–79, <https://doi.org/10.1016/j.tvjl.2007.03.019>, 2008.
- Priya, S. S., Cuce, E., and Sudhakar, K.: A perspective of COVID 19 impact on global economy, energy and environment, *International Journal of Sustainable Engineering*, 14, 1290–1305, <https://doi.org/10.1080/19397038.2021.1964634>, 2021.
- 440 Putt, K. S., Kernick, E. R., Lohse, B. K., Lomboy, J., O'Brien, T., and Pugh, R. B.: The use of chromophore and fluorophore degradation to quantitate UV dose: FD&C dyes as chemical indicators for UV sterilization, *Journal of Microbiological Methods*, 91, 215–221, <https://doi.org/10.1016/j.mimet.2012.08.015>, 2012.
- Reed, N. G.: The History of Ultraviolet Germicidal Irradiation for Air Disinfection, *Public Health Rep*, 125, 15–27, <https://doi.org/10.1177/003335491012500105>, 2010.
- 445 Song, K., Mohseni, M., and Taghipour, F.: Application of ultraviolet light-emitting diodes (UV-LEDs) for water disinfection: A review, *Water Research*, 94, 341–349, <https://doi.org/10.1016/j.watres.2016.03.003>, 2016.
- Terpstra, F. G., Van 't Wout, A. B., Schuitemaker, H., Van Engelenburg, F. A. C., Dekkers, D. W. C., Verhaar, R., De Korte, D., and Verhoeven, A. J.: Potential and limitation of UVC irradiation for the inactivation of pathogens in platelet concentrates, *Transfusion*, 0, 071121030748013-???, <https://doi.org/10.1111/j.1537-2995.2007.01524.x>, 2007.
- 450 Tseng, C.-C. and Li, C.-S.: Inactivation of Virus-Containing Aerosols by Ultraviolet Germicidal Irradiation, *Aerosol Science and Technology*, 39, 1136–1142, <https://doi.org/10.1080/02786820500428575>, 2005.
- Van Dorp, L., Acman, M., Richard, D., Shaw, L. P., Ford, C. E., Ormond, L., Owen, C. J., Pang, J., Tan, C. C. S., Boshier, F. A. T., Ortiz, A. T., and Balloux, F.: Emergence of genomic diversity and recurrent mutations in SARS-CoV-2, *Infection, Genetics and Evolution*, 83, 104351, <https://doi.org/10.1016/j.meegid.2020.104351>, 2020.
- 455 Walker, C. M. and Ko, G.: Effect of Ultraviolet Germicidal Irradiation on Viral Aerosols, *Environ. Sci. Technol.*, 41, 5460–5465, <https://doi.org/10.1021/es070056u>, 2007.
- Wang, C. C., Prather, K. A., Sznitman, J., Jimenez, J. L., Lakdawala, S. S., Tufekci, Z., and Marr, L. C.: Airborne transmission of respiratory viruses, *Science*, 373, eabd9149, <https://doi.org/10.1126/science.abd9149>, 2021.
- 460 Wang, J., Jeevarathinam, A. S., Jhunjhunwala, A., Ren, H., Lemaster, J., Luo, Y., Fenning, D. P., Fullerton, E. E., and Jokerst, J. V.: A Wearable Colorimetric Dosimeter to Monitor Sunlight Exposure, *Adv. Mater. Technol.*, 3, 1800037, <https://doi.org/10.1002/admt.201800037>, 2018.



465 Welch, D., Buonanno, M., Grilj, V., Shuryak, I., Crickmore, C., Bigelow, A. W., Randers-Pehrson, G., Johnson, G. W., and Brenner, D. J.: Far-UVC light: A new tool to control the spread of airborne-mediated microbial diseases, *Sci Rep*, 8, 2752, <https://doi.org/10.1038/s41598-018-21058-w>, 2018.

Zayas, G., Chiang, M. C., Wong, E., MacDonald, F., Lange, C. F., Senthilselvan, A., and King, M.: Cough aerosol in healthy participants: fundamental knowledge to optimize droplet-spread infectious respiratory disease management, *BMC Pulm Med*, 12, 11, <https://doi.org/10.1186/1471-2466-12-11>, 2012.